

# Mechanical Properties of Homopolymer Interfaces: Transition from Simple Pullout To Crazing with Increasing Interfacial Width

Ralf Schnell<sup>†</sup> and Manfred Stamm\*

Max Planck-Institut für Polymerforschung, Postfach 3148, 55021 Mainz, Germany

Costantino Creton\*

Laboratoire de Physico-chimie Structurale et Macromoléculaire, ESPCI, 10 rue Vauquelin, 75231 Paris Cedex 05, France

Received June 1, 1998; Revised Manuscript Received February 16, 1999

**ABSTRACT:** The fracture toughness  $G_c$  of interfaces between several styrene-based homopolymers was investigated by the asymmetric double cantilever beam method while the width of the same interfaces  $a_i$  was investigated in parallel by neutron reflectivity.  $G_c$  was found to be a direct function of  $a_i$  provided that the molecular weights of the homopolymers were sufficiently high. The dependence of  $G_c$  on  $a_i$  could be divided in three regimes: a low toughness regime for  $a_i < 6$  nm, an intermediate regime for  $6 \text{ nm} < a_i < 11$  nm where  $G_c$  increased steeply with  $a_i$  and a plateau regime for  $a_i > 11$  nm where  $G_c$  was independent of  $a_i$ . A molecular analysis of the transition from regime I to II showed that the average interpenetration distance of the homopolymers needed to activate the plastic deformation mechanisms was much less than the average distance between entanglement points in the bulk polymers. This result can be explained by the fact that a significant portion of the load-bearing strands may be loops rather than chain ends, so that an equivalent stress can be sustained by the interface with a much shorter interpenetration distance.

## I. Introduction

Interfaces between polymers play an important role in many polymer applications. This is not only true for adhesives, glues, and coatings but also for polymer blends, where the interfaces are hidden inside the material.

In glassy amorphous polymers, the stress is mainly transferred by entanglements so that a polymer with a number-average molecular weight lower than approximately  $2 M_e$ , where  $M_e$  is the average molecular weight between entanglements, has a negligible fracture toughness. Therefore one expects that the same argument should hold for polymer interfaces; i.e., the fracture toughness  $G_c$  of the interface should be negligible until the chains on both sides of the interface are mutually entangled.

Studies on interfaces between immiscible homopolymers reinforced with block copolymers and with tethered chains have shown that when the interface is able to sustain a stress which is higher than the crazing stress of one of the homopolymers, there is a transition in the failure mechanism from straight chain pullout to crazing.<sup>1–3</sup> In the case of block copolymers where the full length of the block is entangled with its respective homopolymer, the critical stress for the formation of a craze  $\sigma_{\text{craze}}$  can be expressed as a function of the areal density of the copolymer chains  $\Sigma$ , the degree of polymerization  $N$ , and the static monomer friction coefficient of the block being extracted, as shown on Figure 1a. As long as the areal density of copolymer chains is not too high (and the copolymer does not form a dense brush), the transition is predicted to occur when

$$f_{\text{mono}} N \Sigma > \sigma_{\text{craze}} \quad (1)$$

When eq 1 is satisfied, the crack at the interface is preceded by a plastic zone and the fracture toughness is controlled by the failure mechanisms and the stability of that plastic zone. The formation of this plastic zone causes a change in regime of the fracture toughness dependence with  $\Sigma$ , as shown in Figure 1b, from  $G_c \propto \Sigma$  to  $G_c \propto \Sigma^2$  and a numerical increase from a value of a few Joules per square meter to several hundred Joules per square meter.<sup>1,4</sup> Although the derivation of the  $\Sigma^2$  dependence from microscopic arguments is still the matter of some debate,<sup>5,6</sup> its experimental validity is well-established.<sup>7–9</sup>

One expects a similar transition from simple chain pullout to crazing to occur for bare interfaces between homopolymers. However, in this case, it is no longer possible to control independently the areal density of connectors and their length. Historically, the role of entanglements in adhesion between homopolymers has been established for some time: first, by interdiffusion experiments in which the fracture toughness of an interface between two identical polymers has been measured as a function of annealing time above their glass-transition temperature<sup>10,11</sup> and; second, by fracture toughness experiments at the interface between two immiscible polymers.<sup>12,13</sup> In the interdiffusion problem, the fracture toughness  $G_c$  increased with  $t^{1/2}$  and was from the early stages relatively high, whereas for the immiscible polystyrene–poly(methyl methacrylate) interfaces, the fracture toughness was relatively low. However in neither of these cases had a precise measurement of the interfacial width been made on the same samples.

Our previous study,<sup>14</sup> showed that, for homopolymer interfaces between polymers with a sufficiently high molecular weight (with an  $M_n > 8 M_e$ ), there was a direct correlation between the interfacial width, as

\* To whom correspondence should be addressed.

<sup>†</sup> Present address: Akzo Nobel Faser AG, Glanzstoffstrasse, 63785 Oberburg, Germany.

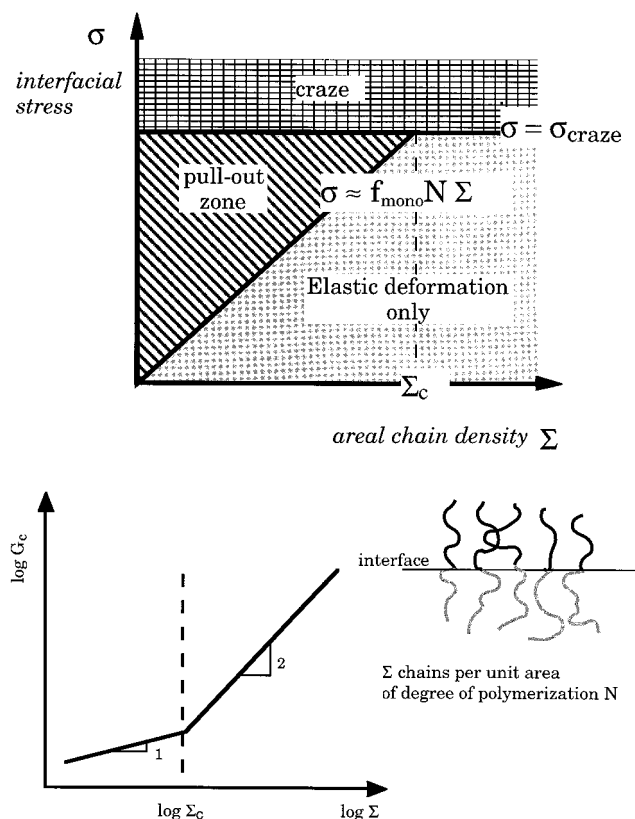


**Figure 1.** (a) Schematics of the interfacial stress as a function of the areal density of connecting chains  $\Sigma$ . For low areal density of chains the failure of the interface, when the interfacial stress is increased, occurs by chain pullout. For areal densities higher than  $\Sigma_c$ , the failure is preceded by the formation of a plastic zone. (b) Schematics of the observed change in regime from  $G_c \propto \Sigma$  to  $G_c \propto \Sigma^2$  when the plastic deformation mechanisms are activated.

measured by neutron reflectivity, and the fracture toughness of the interface as measured by an asymmetric double cantilever beam test. That study was however conducted entirely in the regime where one expects the formation of a craze at the interface.

In this study, we have investigated a wider range of interfacial widths on several interfaces between different glassy polymers and have demonstrated the existence of a similar transition from simple chain pullout to crazing which is now observed for a critical value of interfacial width.

To explore a range of interfacial widths without altering much the mechanical properties of the bulk polymers, we have worked with three different (miscible and immiscible) experimental systems: the polystyrene–polystyrene (PS–PS) interfaces for the larger values of interfacial width (in this case, the interfacial width is controlled by the time allowed for chain interdiffusion), the polystyrene–poly(*p*-methylstyrene) (PS–PpMS) interfaces for intermediate values of interfacial width ( $\chi \approx 0.0035$ – $0.0055$ ), and the statistical copolymer of poly(bromostyrene–styrene)–polystyrene (PBr<sub>x</sub>S–PS) interfaces for the low values of interfacial width ( $\chi \approx 0.1$ – $0.001$ ).

Although directly comparing the fracture toughness results of interfaces between different bulk polymers is not generally possible or advisable (the fracture toughness is dependent on the bulk properties of the polymers on either side of the interface), we feel that it is reasonable to do it in the present study for the following reasons:

**Table 1. Molecular Weights of Polystyrenes and Poly(*p*-methylstyrenes) Used in both NR and Fracture Tests**

| polymer                         | $M_W$ [kg/mol] | $M_W/M_N$ |
|---------------------------------|----------------|-----------|
| polystyrene:                    |                |           |
| PS139k                          | 139.4          | 1.04      |
| PS310k                          | 309.6          | 1.03      |
| PS862k                          | 861.7          | 1.10      |
| PS1,25M                         | 1250.7         | 1.11      |
| <i>d</i> PS110k                 | 110            | 1.06      |
| <i>d</i> PS714k                 | 714.3          | 1.04      |
| poly( <i>p</i> -methylstyrene): |                |           |
| PpMS131k                        | 131            | 1.05      |
| PpMS157k                        | 157.1          | 1.06      |
| PpMS570k                        | 569.6          | 1.14      |
| PpMS613k                        | 613.1          | 1.11      |

**Table 2. Molecular Weights of the Brominated Polymers Used for the Neutron Reflectivity Results (from ref 26)**

| polymer                              | $x$  | $M_W$ [kg/mol] | $M_W/M_N$ |
|--------------------------------------|------|----------------|-----------|
| <i>d</i> -Polystyrene ( <i>d</i> PS) | 0    | 158            | <1.2      |
| PBr <sub>x</sub> S                   | 0.16 | 158            | <1.2      |
| PBr <sub>x</sub> S                   | 0.19 | 158            | <1.2      |
| PBr <sub>x</sub> S                   | 0.23 | 158            | <1.2      |
| PBr <sub>x</sub> S                   | 0.28 | 158            | <1.2      |
| PBr <sub>x</sub> S                   | 1    | 158            | <1.2      |

**Table 3. Molecular Weights of the Brominated Polymers Used for the Fracture Toughness Experiments**

| polymer            | $x$  | $M_W$ [kg/mol] | $M_W/M_N$ |
|--------------------|------|----------------|-----------|
| Polystyrene (PS)   | 0    | 139            | 1.04      |
| PBr <sub>x</sub> S | 0.11 | 190            | 1.11      |
| PBr <sub>x</sub> S | 0.18 | 134            | 1.03      |
| PBr <sub>x</sub> S | 0.27 | 157            | 1.07      |
| PBr <sub>x</sub> S | 0.33 | 166            | 1.11      |
| PBr <sub>x</sub> S | 1    | 145            | 1.04      |

(1) The crazing stresses of all of these styrene-based polymers are not too different from those of PS. Therefore, one does not expect, for a given interfacial width, very different plastic deformation mechanisms close to the crack tip when going from one polymer system to another.

(2) With the geometrical parameters which we used, no significant amounts of crack deviations from the main interface (due to crack propagation in mixed mode<sup>15,16</sup>) were seen at the interface, suggesting therefore that the values of fracture toughness that we measured were sensitive to the molecular structure of the interface and that the fracture toughness results could quantitatively be compared.

(3) The molecular weights of the polymers we used were all above  $8 M_e$ . In this regime, the fracture toughness of the bulk PS polymer is no longer molecular-weight dependent, and we expect that the interfacial fracture toughness will not be sensitive to that parameter.

## II Experimental Section

**II.1. Materials.** The polymers were all synthesized by anionic polymerization (Max-Planck Institut für Polymerforschung). Their molecular weights have been characterized by gel permeation chromatography using PS standards. Three types of interfaces were tested: PS/PS interfaces, PS/PpMS interfaces and PS/PBr<sub>x</sub>S interfaces. The respective characteristics of the polymers used are listed in Tables 1–3. Deuterated polystyrene, *d*PS is used only for the neutron reflectivity studies. For the PS/PS and PS/PpMS studies, polymers with identical molecular weights were used for the NR and the fracture studies. However, this was not possible for the PS/PBr<sub>x</sub>S interfaces because of the large amounts of polymer

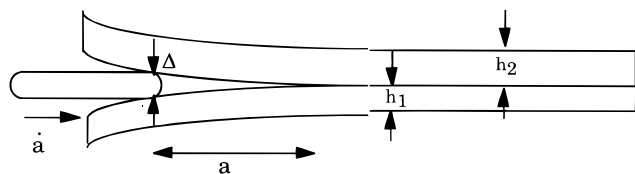


**Figure 2.** Schematic drawing of the ADCB-test geometry and of the important parameters defined in the text.

**Table 4. Representative Mechanical Properties of the Polymers Used for the Fracture Toughness Experiments**

| polymer                               | Young's modulus [GPa] | crazing stress [MPa] |
|---------------------------------------|-----------------------|----------------------|
| PBr <sub>x</sub> S ( <i>x</i> = 0.11) | 2.8                   | 48                   |
| PBr <sub>x</sub> S ( <i>x</i> = 0.11) | 2.6                   | 44                   |
| PS 1M                                 | 2.4                   | 48                   |
| PpMS                                  | 2.1                   | 31                   |

needed for the fracture experiments. PBr<sub>x</sub>S is a statistical copolymer of poly(styrene-*co-p*-bromostyrene), where the degree of bromination *x* is obtained by chemical analysis. Molecular weights refer to the molecular weight of PS prior to bromination. The glass transition *T<sub>g</sub>* is estimated from differential scanning calorimetry (heating rate, 10 deg/min).

Because we have performed mechanical tests, the elastic modulus and the crazing stress of the different polymers were also measured using a 3-point bending method<sup>7</sup> and are listed in Table 4. Ideally, the average molecular weight between entanglements would also be needed for the different polymers; however, we took for all of our analyses, the values which are known for PS.

The average distance between entanglement points *d* can be evaluated using the relation<sup>17</sup>

$$d^2 = C_{\infty} l_0^2 M_e m_0^{-1} \quad (2)$$

where *C<sub>∞</sub>* = 10.5 for PS,<sup>17</sup> *M<sub>e</sub>* is the average molecular weight between entanglement points (18 000 for PS<sup>18</sup>), *m<sub>0</sub>* is the molar mass per backbone bond (52 for PS), and *l<sub>0</sub>* is the length of a C–C bond (1.54 Å).

**II.2. Fracture Toughness Tests. PS/PpMS:** PS and PpMS were separately compression-molded at 160 °C into sheets (5 cm × 4 cm) with respective thicknesses of 2 and 3 mm. To obtain the sandwich samples, the PpMS and PS sheets were joined together in one mold and annealed at variable temperatures under slight pressure to obtain contact between the sheets. To ensure that the annealing time was long enough to reach equilibrium, comparable samples were annealed for different times. Samples were quenched to room temperature by putting the hot mold between two thick metal plates. These sandwich samples were then cut into 0.8 cm × 5 cm strips. Different annealing temperatures and molecular weights were used to obtain different interfacial widths.<sup>14</sup>

**PS/PS:** PS sheets were prepared in a similar way except that they had an identical thickness of 2 mm. The annealing times for the sandwich samples were varied between 5 and 95 h, and the annealing temperatures were varied between 125 and 180 °C to obtain a distribution of interfacial widths.<sup>14</sup>

**PS/PBr<sub>x</sub>S:** Instead of the ADCB geometry, a trilayer A–B–A geometry was chosen, where a thin (10–20 μm) solvent-cast PBr<sub>x</sub>S film is embedded between two 2 mm PS sheets.

The fracture toughness measurements between PS and PpMS were performed using an asymmetric double cantilever beam (ADCB) as shown in Figure 2. For the PS/PS and the PS/PBr<sub>x</sub>S interfaces, a mechanically symmetric geometry was used.

In the latter case, because a thin Pbr,S film is put between two thick PS sheets, the crack propagates at one of the interfaces between the PS and the PBr<sub>x</sub>S. Because the plastic deformation occurred in the thick PS phase, we were insensitive to the precise thickness of the PBr<sub>x</sub>S layer.<sup>19</sup> This symmetric geometry was chosen to avoid an optimization of

the phase angle for every single degree of bromination. Because very little or no crack kinking away from the interface occurred and no significant jump of the crack from one interface to the other took place, we can assume that the measured *G<sub>c</sub>* is representative of the toughness of the interface. The samples were annealed at 122 °C for up to 3 days.

To determine the fracture toughness of polymer–polymer interfaces, a razor blade was inserted and pushed into the interface at a constant speed of 5 μm/s. The dependence of the fracture toughness on crack velocity was investigated in the range between 1 and 150 μm/s. As no significant dependence was observed, we assumed that the measured energy release rate at 5 μm/s was equal to *G<sub>c</sub>*, the critical energy release rate at zero velocity. The resulting crack length was measured in situ using a video camera. To calculate *G<sub>c</sub>* from the crack length *a*, we used the expression proposed by Creton et al.<sup>7</sup> based on the beam on an elastic foundation model.<sup>20</sup> This analysis empirically takes into account the finite elasticity of the material ahead of the crack tip and has been shown to give reliable results for polymer interfaces:

$$G_c = \frac{3\Delta^2}{8a^4} \frac{E_1 h_1^3 E_2 h_2^3}{E_1 h_1^3 \alpha_2^2 + E_2 h_2^3 \alpha_1^2} \quad (3)$$

The parameters *h*, *a*, and *D* are described in Figure 2. *E<sub>i</sub>* is the Young's modulus, and *a<sub>i</sub>* is the respective correction factor for the material *i*:

$$\alpha_i = \frac{(1 + 1.92h_i/a) + [1 + 1.22(h_i/a)^2] + [1 + 0.39(h_i/a)^3]}{(1 + 0.64h_i/a)}$$

**II.3. Neutron Reflectivity Experiments.** Thin polymer films (80–100 nm) were prepared by spin coating from a solution of the respective polymers in toluene onto silicon or float glass substrates. The obtained films were characterized by phase interference microscopy and X-ray reflectometry in terms of roughness and thickness. For the preparation of the double layers, one film was floated off the substrate onto a deionized water surface and picked up by a second film which was still on a substrate. After drying several days under vacuum at ambient temperature, the double layer sample was investigated again with interference microscopy and X-ray reflectometry. After the precharacterization of the samples, neutron reflectivity experiments were performed on the neutron reflectometer TOREMA II at GKSS in Geesthacht, Germany. A fixed wavelength of 4.3 nm (graphite monochromator) at variable incident angle was employed. A position-sensitive BF<sub>3</sub>-detector was used for the investigations.

Neutron reflectivity allows in a nondestructive way the determination of interfacial widths (*a<sub>i</sub>*) in the range between 2 and 30 nm with a resolution better than 0.5 nm.<sup>21</sup> This method is sensitive to gradients of the refractive index *n*,

$$n = 1 - \frac{\lambda^2}{2\pi} N_b \quad (4)$$

where *λ* is the wavelength of the neutron beam and *N<sub>b</sub>* is the scattering length density of the polymer. The absorption is neglected in this formula.

Because of the large difference in scattering length between hydrogen and deuterium, it is possible to obtain sufficient contrast between the layers by using a deuterated film. The reflectivity data was analyzed with a model-dependent fitting procedure based on a matrix algorithm described by Lekner.<sup>22</sup> In agreement with mean field theory for a concentration-independent *χ*-parameter, we used a tanh-shaped interfacial profile to describe the volume fraction (*φ*) profile for the simulation of the reflectivity curves

$$\phi(z) = 1/2 \left[ (\phi_1^B + \phi_2^B) + (\phi_1^B - \phi_2^B) \tanh\left(\frac{2(z - z_0)}{a_i}\right) \right] \quad (5)$$

where *z<sub>0</sub>* is the center of the interface and *φ<sub>1</sub><sup>B</sup>* and *φ<sub>2</sub><sup>B</sup>* are the



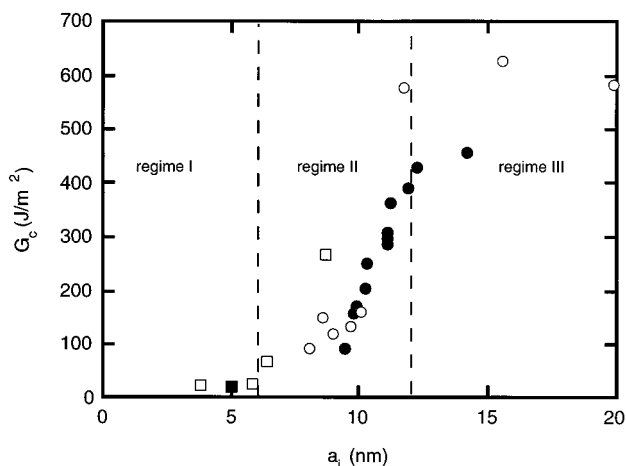


**Figure 3.** Fracture toughness  $G_c$  of different samples plotted as a function of the interfacial width  $a_i$ :  $\square$  PS-PBr<sub>x</sub>S interfaces;  $\blacksquare$  PS-PMMA interfaces (data from refs 28 and 29)  $\bullet$  PS-PPMS interfaces; and  $\circ$  PS-PS interfaces. Regime I, II, and III are discussed in the text.

bulk volume fractions of the components. The measured interface width has been corrected for initial interfacial roughness and capillary waves as described previously.<sup>23</sup> Because the interface width is relatively large, it can be shown<sup>24</sup> that the capillary wave contribution as calculated from theory<sup>25</sup> becomes relatively small.

For the neutron reflectivity experiments, a deuterated film is always used, whereas for the fracture toughness tests, only protonated materials are taken.

**II.4. Matching Neutron Reflectivity Results with Fracture Toughness Results.** One of the main goals of this study was to compare directly the fracture toughness and interfacial width of interfaces with identical structures. Therefore, ideally, one would have used the same polymers for the fracture toughness and the NR experiments. However, because of the large amounts of polymer necessary to do fracture toughness experiments, this was not done for the PS/PBr<sub>x</sub>S interfaces. In this case, the interfacial width for the degree of bromination used in fracture tests was extrapolated from the data of Guckenbiehl et al.<sup>26</sup> on a polymer series with very similar molecular weights using an empirically determined expression for the dependence of the interfacial width on the interaction parameter  $\chi$  between PS and PBr<sub>x</sub>S.<sup>27</sup>

$$a_i = \frac{2b}{\sqrt{6(\chi_{S/BrS}\phi_{Br}^s - 0.0017)}} \quad (6)$$

where  $\phi_{Br}$  is the volume fraction of BrS in the PBr<sub>x</sub>S and  $\chi_{S/BrS}$  is the monomer interaction parameter between styrene and 4-bromostyrene. At 122 °C,  $\chi_{S/BrS} = 0.095$ .<sup>27</sup>

### III. Results and Discussion

Figure 3 shows the fracture toughness  $G_c$  versus the interfacial width  $a_i$  for our different polymer systems. The first observation is that there seems to be a good correlation between the interfacial width and the fracture toughness even though the experimental systems are different. One does not expect this to be true in general, but in this case it is due to the following facts: (1) All molecular weights used are much higher than the average molecular weight between entanglements of the respective polymers in the bulk. (2) All of our experimental systems are styrene-based, deform by crazing at the crack tip, and have comparable crazing stresses. (3) Molecular parameters such as Kuhn length and average molecular weight between entanglements are not significantly different for all investigated materials.

The dependence of the fracture toughness on the interfacial width can be divided in three different regimes resulting in a S-shaped curve:

**Regime I.** At low interfacial widths (<6 nm), the fracture toughness was found to be rather low, and no steep increase was found with increasing interfacial widths in this regime. The existence of this regime had been suggested because the fracture toughness of the interfaces between PS and PpMS, which increases linearly with  $a_i$  for 9 nm <  $a_i$  < 12 nm, did not extrapolate (at zero toughness) to a vanishing interfacial width.<sup>14</sup> We have also added as a comparison, the value of fracture toughness and interfacial width for the PS-PMMA interface.<sup>28,29</sup>

**Regime II.** At intermediate interfacial widths (6–11 nm), a steep increase of the fracture toughness is observed.

**Regime III.** At higher values of interfacial width, the fracture toughness nearly reaches the bulk toughness. The main evidence for this regime is the fact that the crack often kinked out of the interface during the ADCB test. This is why it was only possible to obtain data points in a few cases in this third regime.

The dependence of  $G_c$  on interfacial width in regime II and the transition from regime II to III have been discussed by Schnell et al.<sup>14</sup> and can be summarized as follows:

At intermediate values of  $a_i$ , the polymer chains on either side of the interface begin to form mechanically effective entanglements and a plastic zone is formed ahead of the crack tip during crack propagation. Chain scission inside the plastic zone becomes an increasingly dominant failure mechanism with increasing interfacial width and a steep increase of the fracture toughness of the interface is observed. It should be noted that the exact functional dependence of  $G_c$  on  $a_i$  is difficult to establish because of the high level of scatter of the data.

At a certain level of the interfacial width (>12 nm for our system), the interdiffusing polymer chains are able to form entanglements which are mechanically as effective as in the bulk phase, and the fracture toughness reaches a maximum level. This interfacial width corresponds roughly to the average distance between mechanically effective entanglement points in PS (9.3 nm) but is much shorter than the radius of gyration of the polymers (for example, 21.3 nm for 570k PS), which could imply that the polymer chain needs only to interpenetrate roughly by an entanglement distance to provide an optimum adhesion. Clearly, this analysis should be verified with other systems and is not expected to be valid for lower molecular weights where the fracture toughness will be a function of a combination of interfacial width and molecular weight.

However, this result should be contrasted with what has been found for the mechanical effectiveness of end-tethered chains (block copolymers or grafted chains) at interfaces where an interpenetration distance with the bulk polymer of several entanglement lengths was necessary to obtain the maximum fracture toughness.<sup>2,3,7</sup> In this case, the interfacial width between the tethered chain and the homopolymer is controlled almost exclusively by the molecular weight of the tethered chain, and a molecular weight of 4–5  $M_e$  was found to give an optimal toughness.<sup>2,3</sup>

The focus of the present paper however is to discuss the transition from regime I to II. From our data, there appears to be a sharp increase, which is more evident

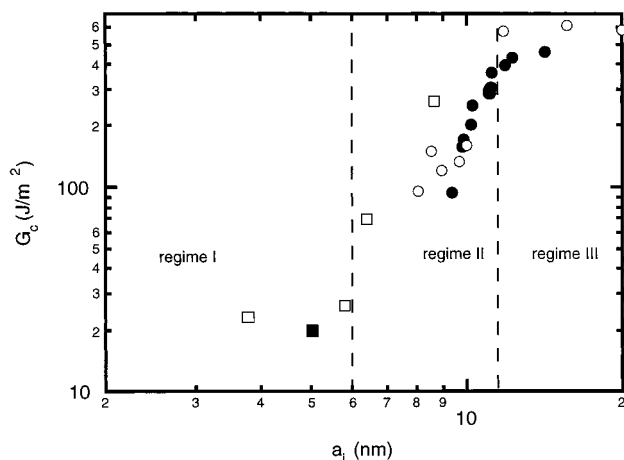


**Figure 4.** Log-log plot of the fracture toughness  $G_c$  as a function of the interfacial width  $a_i$  showing the transition from simple chain pullout to crazing (regimes I–II):  $\square$  PS–PBr,S interfaces;  $\blacksquare$  PS–PMMA interfaces (data from refs 28 and 29);  $\bullet$  PS–PPMS interfaces; and  $\circ$  PS–PS interfaces.

in the log-log plot in Figure 4 with  $G_c$  around  $a_i \approx 6$  nm. Based on the knowledge of crack propagation at similar interfaces reinforced with block copolymers, this discontinuity should be caused by the formation of a plastic zone at the crack tip when the stress at the interface exceeds the crazing stress of one of the two homopolymers. It may be surprising at first sight that this transition occurs for an interpenetration distance clearly lower than the average distance between entanglement points (9.3 nm for PS), and it is interesting to examine why this can be so.

If below the transition the main fracture mechanism is chain pullout, then, using the same argument which led to eq 1, one can write

$$f_{\text{mono}} \bar{N} \bar{\Sigma} = \sigma_{\text{craze}} \quad (7)$$

where  $f_{\text{mono}}$  is a static monomer friction coefficient,  $\bar{N}$  is an average interpenetration length and  $\bar{\Sigma}$  an average areal density of load-bearing strands at the transition from chain pullout to crazing.

However, although for block copolymers the values of  $\bar{N}$  and  $\bar{\Sigma}$  can be independently controlled and are well-defined (leading to a good estimate of  $f_{\text{mono}}$ ),<sup>1,3</sup> this is no longer the case for  $\bar{N}$  and  $\bar{\Sigma}$  and for interfaces between homopolymers.  $\bar{N}$  will be the average length of the polymer strands being extracted during a disentanglement from the polymer on the opposite side of the interface and  $\bar{\Sigma}$  will be the average number per unit area of those strands being extracted.

One can obtain nevertheless an estimate of the product  $\bar{N} \bar{\Sigma}$  which is necessary to activate the plastic deformation processes at the crack tip. With  $\sigma_{\text{craze}} \approx 48$  MPa for PS and  $f_{\text{mono}} \approx 6 \times 10^{-12}$  N, as estimated from the pullout of tethered PS chains,<sup>1</sup> one obtains  $\bar{N} \bar{\Sigma} \approx 8 \times 10^{18} \text{ m}^{-2}$ . This value is the total number of monomers per unit area of interface that are experiencing a friction force. However, to further interpret this result, one must point out that, unlike the situation where a tethered chain is being extracted from a homopolymer matrix,<sup>1</sup> the chains are here being extracted from themselves (or rather from the homopolymer chains on the other side of the interface). Furthermore, this value could be significantly smaller if a more efficient friction mecha-

nism (chain scission or friction of loops) is present, as will be discussed below.

Let us examine now two limiting cases leading to the formation of a plastic zone:

(1) The chains are sufficiently entangled with each other so that the only failure mechanism is chain scission. In this case, the force necessary to fracture a C–C bond has been estimated<sup>7</sup> to be 1 nN and in order to reach the crazing stress, the areal density of strands would be  $\bar{\Sigma} \sigma_{\text{craze}} / l_0 = 0.46 \times 10^{17} \text{ m}^{-2} = 0.046 \text{ strands/nm}^2$ .

(2) The chains are not mutually entangled and fail exclusively by chain pullout. If one assumes that the chains at the interface are Gaussian, one can obtain an average interpenetration length given by

$$\bar{N} \approx \frac{a_i^2}{2 C_{\infty} l_0} \quad (8)$$

which would give for PS an average value of  $\bar{N} = 72$  monomers. If this value of  $\bar{N}$  is then replaced in eq 7, one obtains for the areal density of effective strands  $\bar{\Sigma} \approx 1.1 \times 10^{17} \text{ m}^{-2} = 0.11 \text{ strands/nm}^2$ .

These two results should be compared with the value of  $\Sigma_{\text{bulk}}$  in the bulk polymer which can be obtained by the relation

$$\Sigma_{\text{bulk}} = \frac{\nu d}{2} = \frac{1 \rho N_A (C_{\infty} \bar{M}_e)^{1/2}}{2 M_e} l_0 = \frac{\rho N_A l_0}{2} \left( \frac{C_{\infty}}{M_e m_0} \right)^{1/2} \quad (9)$$

where  $\rho$  is the density of the polymer and  $N_A$  is Avogadro's number. Using the standard values for polystyrene, one obtains  $\Sigma_{\text{bulk}} \approx 1.6 \times 10^{17} \text{ m}^{-2}$ .

Although the entanglement structure and chain conformation near an interface is not precisely known,  $\Sigma_{\text{bulk}}/2$  should be a reasonable estimate for the average areal density of load-bearing strands because this would imply that half of the strands are being extracted from the other half. Comparing this value with the estimates obtained with our two models, we can now propose a tentative molecular picture of the fracture toughness of polymer interfaces between homopolymers.

If a mechanism of pure chain pullout of chain ends was active, the average number of strands necessary to sustain a stress high enough to form a plastic zone would be unrealistically high. On the other hand, if all chains failed by scission, the areal density of strands at the transition would be low. This implies that a fraction of chains are entangled and fail by either a more effective friction mechanism or scission while another fraction of chains are not entangled and fail by chain pullout. In other words, the mechanical response which we observe is consistent with a distribution of values of extracted  $N$ s across the interface which is not Gaussian (i.e., continuous) but rather bimodal. A small fraction of strands may be bearing most of the stress in this regime.

Again, it is interesting to contrast this behavior with that of end-tethered chains being extracted from a homopolymer. In that case, all tethered chains are fully extracted, and there is no distribution of extracted  $N$ s (as long as  $\Sigma$  is not too high). To obtain a plastic deformation zone, a molecular weight of the tethered chain of at least  $N_e$  is necessary. The use of such a molecular weight implies an interfacial width between the tethered chain and the homopolymer of the order of the distance between entanglement points.<sup>30</sup>

If the value of  $a_i$  increases beyond the transition, one would expect the proportion of chains failing by chain scission to increase through most of the regime II described above. Only in regime III would the plastic zone fail by chain scission exclusively and become therefore independent of the interpenetration distance.

To qualify the generality of this picture, several comments should be made.

(1) Molecular simulations have shown that in the strong segregation limit the chains near an interface are not Gaussian but have a shorter radius of gyration in the direction perpendicular to the interface.<sup>31</sup> For a given interfacial width, this would increase the average interpenetration degree of polymerization and favor chain scission relative to chain pullout.

(2) Real homopolymer chains at interfaces might also disentangle in bundles rather than individually. Therefore, the use of the single-strand monomer friction coefficient would lead to an underestimate of the product  $\bar{N}\bar{\Sigma}$ . The magnitude of this effect will increase with the interaction parameter  $\chi$  so that one would not necessarily expect to find the same critical value of  $a_i$  for a PS/PS interface as for a PBr<sub>s</sub>S-PS interface, for example. Unfortunately, it is experimentally difficult to obtain a mechanically testable PS-PS interface with an interfacial width below 8 nm.

(3) Finally, in our investigation, we have used polymers with very similar bulk elastic and plastic deformation properties. A systematic investigation of the effect of the width of the interface is only possible in those conditions. If the bulk properties of the polymers are too different, the effect of the interface can be masked completely by bulk effects.

#### IV. Conclusions

The fracture toughness of interfaces between high-molecular-weight polymers ( $M > 8M_c$ ) with comparable mechanical properties increases with interfacial width within three different regimes: in the first regime, the interface fails by simple chain pullout and gives a low interfacial toughness. At a critical value of  $a_i$ , a plastic zone forms ahead of the interface and  $G_c$  increases more rapidly with  $a_i$ . Interestingly this transition occurs for an interpenetration distance  $a_i$  shorter than the average distance between entanglements in the bulk polymer. At the molecular level, this transition can be translated into a critical value of the product of an average interpenetration degree of polymerization  $\bar{N}$  and an average areal density of load-bearing strands  $\bar{\Sigma}$ .

Comparison of the values of  $\bar{\Sigma}$  that can be inferred from our data with the areal density of strands in the bulk polymer suggests that a significant part of the load-bearing strands crossing the interface are actually loops rather than chain ends and fail by chain scission rather than chain pullout. This is consistent with a distribution of interpenetration lengths  $N$  which would be bimodal rather than continuous, leading therefore to a fracture toughness which does not increase in a straightforward way with the average interfacial width obtained with neutron reflectivity profiles. Clearly, more information on the topology of the chains at the interface (and not only on the distribution of monomers) is needed to confirm this analysis.

Once the plastic deformation at the interface is activated, both  $\bar{N}$  and  $\bar{\Sigma}$  increase to the bulk value with increasing interfacial width  $a_i$  and cause a sharp increase in  $G_c$ . In that regime, a plastic zone is always formed, and the molecular fracture mechanism of the

plastic zone probably shifts progressively from partial chain pullout to chain scission until  $G_c$  no longer increases with  $a_i$ . The transition to this last regime requires an interpenetration distance larger than the average distance between entanglement points in the bulk.

An important conclusion of this study is that a small local decrease in the segment interaction causing an increased interpenetration between homopolymers can be very effective in increasing the fracture toughness of an interface, because a moderate amount of interpenetration is required between homopolymers to reach high values of  $G_c$ . This could explain the reported high mechanical effectiveness of random copolymers (relative to block copolymers) at interfaces,<sup>32-35</sup> as well as the effectiveness of solvent welding of polymers.

#### References and Notes

- (1) Washiyama, J.; Kramer, E. J.; Hui, C. Y. *Macromolecules* **1993**, *26*, 2928.
- (2) Norton, L. J.; Smigolova, V.; Pralle, M. U.; Hubenko, A.; Dai, K. H.; Kramer, E. J.; Hahn, S.; Berglund, C.; DeKoven, B. *Macromolecules* **1995**, *28*, 1999.
- (3) Sha, Y.; Hui, C. Y.; Kramer, E. J.; Hahn, S. F.; Berglund, C. A. *Macromolecules* **1996**, *29*, 4728.
- (4) Creton, C.; Brown, H. R.; Deline, V. R. *Macromolecules* **1994**, *27*, 1774.
- (5) Brown, H. R. *Macromolecules* **1991**, *24*, 2752.
- (6) Wool, R. P. *Polymer Interfaces*, 1st ed.; Hanser Verlag: Munich, 1995.
- (7) Creton, C.; Kramer, E. J.; Hui, C. Y.; Brown, H. R. *Macromolecules* **1992**, *25*, 3075.
- (8) Char, K.; Brown, H. R.; Deline, V. R. *Macromolecules* **1993**, *26*, 4164.
- (9) Boucher, E.; Folkers, J. P.; Hervet, H.; Léger, L.; Creton, C. *Macromolecules* **1996**, *29*, 774.
- (10) Jud, K.; Kausch, H. H.; Williams, J. G. *J. Mater. Sci.* **1981**, *16*, 204.
- (11) Wool, R. P.; Yuan, B. L.; McGarel, O. J. *Polym. Eng. Sci.* **1989**, *29*, 1340.
- (12) Foster, K. L.; Wool, R. P. *Macromolecules* **1991**, *24*, 1397.
- (13) Willett, J. L.; Wool, R. P. *Macromolecules* **1993**, *26*, 5336.
- (14) Schnell, R.; Stamm, M.; Creton, C. *Macromolecules* **1998**, *31*, 2284.
- (15) Xiao, F.; Hui, C.-Y.; Washiyama, J.; Kramer, E. J. *Macromolecules* **1994**, *27*, 4382.
- (16) Xiao, F.; Hui, C. Y.; Kramer, E. J. *J. Mater. Sci.* **1993**, *28*, 5620.
- (17) Xu, Z.; Hadjichristidis, N.; Fetters, L. J.; Mays, J. W. *Adv. Polym. Sci.* **1995**, *120*, 1.
- (18) Onogi, S.; Masuda, T.; Kitagawa, K. *Macromolecules* **1970**, *3*, 109.
- (19) Passade, N.; Creton, C. to be published.
- (20) Kanninen, M. F. *Int. J. Fract.* **1973**, *9*, 83.
- (21) Stamm, M.; Schubert, D. W. *Annu. Rev. Mater. Sci.* **1995**, *25*, 325.
- (22) Lekner, J. *Theory of Reflection*; Martinus Nijhoff: Dordrecht, 1987.
- (23) Schubert, D. W.; Stamm, M. *Europhys. Lett.* **1996**, *35*, 419.
- (24) Schnell, R. Ph.D. Thesis, University of Mainz, Mainz, 1997.
- (25) Semenov, A. N. *Macromolecules* **1994**, *27*, 2732.
- (26) Guckenbiehl, B.; Stamm, M.; Springer, T. *Physica B* **1994**, *198*, 127.
- (27) Schubert, D. W. Thesis, University of Mainz, Mainz, 1997.
- (28) Anastasiadis, S. H.; Russell, T. P.; Satija, S. K.; Majkrzak, C. F. *J. Chem. Phys.* **1990**, *92*, 5677.
- (29) Brown, H. R. *J. Mater. Sci.* **1990**, *25*, 2791.
- (30) Shull, K. R. *J. Chem. Phys.* **1991**, *94*, 5723.
- (31) Müller, M.; Binder, K.; Oed, W. *J. Chem. Soc., Faraday Trans.* **1995**, *91*, 2369.
- (32) Dai, C. A.; Osuji, C. O.; Jandt, K. D.; Dair, B. J.; Ober, C. K.; Kramer, E. J. *Macromolecules* **1997**, *30*, 6727.
- (33) Bernard, B.; Brown, H. R.; Russell, T. P.; Hawker, C. J. *Polym. Mater. Sci. Eng.* **1996**, *29*, 155.
- (34) Kulasekera, R.; Kaiser, H.; Ankner, J. F.; Russell, T. P.; Brown, H. R.; Hawker, C. J.; Mayes, A. M. *Macromolecules* **1996**, *29*, 5493.
- (35) Sikka, M.; Pellegrini, N. N.; Schmitt, E. A.; Winey, K. I. *Macromolecules* **1997**, *30*, 445.